2008 IEEE International Conference on
Robotics and Automation
Pasadena, CA, USA, May 19-23, 2008

Design and Control of a Multifunction Myoelectric Hand with New Adaptive Grasping and Self-locking Mechanisms

Jun-Uk Chu, *Member, IEEE*, Dong-Hyun Jung, and Yun-Jung Lee, *Member, IEEE*

***Abstract*—This paper presents a multifunction myoelectric hand that is designed with underactuated mechanisms. The finger design allows an adaptive grasp, including adaptation between fingers and phalanges with respect to the shape of an object. In addition, a self-lock is embedded in the metacarpo-phalangeal joint to prevent back driving when external forces act on the fingers. The thumb design also provides adaptation between phalanges and adds an intermittent rotary motion to the carpometacarpal joint. As a result, the hand can perform versatile grasping motions using only two motors, and is capable of natural and stable grasping without complex sensor and servo systems. Moreover, the adaptive grasping capabilities reduce the requirements of electromyogram pattern recognition, as analogous motions, such as cylindrical and tip grasps, can be classified as one motion.**

I. Introduction

A MYOELECTRIC hand is an upper-limb prosthesis that consists of several parts: kinematics, actuators, control, sensors, and an electromyogram (EMG)-based interface. While conventional myoelectric hands, such as the Otto Bock Hand or Motion Control Hand, have a good reliability and robustness, their mechanism of two rigid fingers and a rigid thumb linked in opposition by a lever and simultaneously actuated by a single motor is unable to adapt to different object sizes and shapes and only allows a tip-to-tip pinch grasp with a few contact points. Thus, a high pinch force is required to obtain a stable grasp, and objects must be grasped accurately. The EMG-based interface allows the myoelectric hand to recognize the user's intention by comparing the mean absolute value of the EMG signal to a predetermined threshold based on the fact that the amplitude of the EMG signal is almost proportional to the level of muscle activity, allowing the generation of a few control commands, such as open/grasp or pronation/supination.

However, recent research has developed various multi-function myoelectric hands to overcome the limitations of the conventional models. Essentially, these multifunctional hands use a design approach based on underactuated mechanisms, where the number of motors is lower than the degrees of freedom. Plus, underactuated mechanisms can facilitate *adaptive grasping*, allowing the fingers and thumb to adapt to the shape of a grasped object to increase the contact points between the hand and the object [1]. Thus, underactuated hands combine the advantages of being light weight and small in size, while retaining the grasping capabilities of independent actuated hands.

For example, Dechev *et al.* [1] developed an under-actuated hand with a cylinder spring mechanism that allows the four fingers and thumb to flex inward independently to conform to the shape of an object. The linear motion of the cylinder spring is achieved by a lead screw and ball nut. However, each finger is comprised of six links and cannot provide adaptation among the phalanges. Also, the motor system is located in the forearm due to the volume required by the cylinder spring mechanism. Similarily, Kyberd *et al.* [2] proposed a whiffle-tree mechanism for the index and middle fingers to achieve adaptive grasping. Yet, the four-bar mechanism of each finger only provides a fixed curling trajectory. More recently, Carrozza *et al.* [3] proposed an adaptation mechanism among fingers and phalanges, where each finger includes cables and compression springs, and each cable is fixed to a corresponding phalanx through each spring. When one link contacts an object, the compression of the corresponding spring allows the other links to continue bending. A linear slider with three pulleys drives all the cables for the fingers, and three pairs of cables for the index and middle fingers are wrapped around the respective pulley to provide adaptation among the fingers. However, the grasping force is limited to 10 N, as a portion of the motor's power is consumed by the compression of the springs. Another drawback of a spring mechanism is that when the spring is not fully compressed by the slider to an intermediate position, the fingers can be back-driven by external forces.

Accordingly, to improve the capability of adaptive grasping, an innovative adaptation mechanism is proposed using a spiral spring and cam-ball mechanism. The winding of the spiral spring provides adaptation between the fingers in the restricted volume of the metacarpophalangeal joint, where an embedded cam-ball mechanism guarantees the self-locking of each finger. Using this mechanism, a multifunction myoelectric hand, called the KNU (Kyungpook National University) hand, is presented, which is composed of four pairs of spiral springs, cams, and balls; four fingers capable of adaptation between the phalanges; and a thumb with the movements of adduction/abduction and flexion/extension. This paper describes the design of the KNU hand, and presents experimental results when the hand is controlled by EMG signals.

Manuscript received Sept. 14, 2007. This work was supported by the Korea Research Foundation Grant funded by the Korean Government (MOEHRD, Basic Research Promotion Fund) (KRF-2006-311-D00655).

J. U. Chu, D. H. Jung, and Y. J. Lee are with the School of Electrical Engineering and Computer Science, Kyungpook National University, Daegu, Korea (phone: +82-53-950-6562; fax: +82-53-950-5505; e-mail: juchu@ee.knu.ac.kr; dhjung@ee.knu.ac.kr; yjlee@ee.knu.ac.kr).

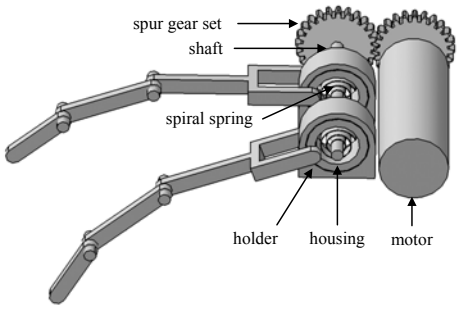

Fig. 1. Spiral spring mechanism for shape adaptation between fingers.

II. Design of KNU Hand

The KNU hand is a five-fingered myoelectric hand, and the design concept includes three functional features: first, the four fingers allow shape adaptation and self-locking; second, for each finger, the three phalanges can flex independently to wrap an object with multi-point contacts; and third, the thumb also has three adaptive phalanges and performs adduction and abduction. In addition, the number of motors is limited to only two, and they are placed in the palm. To realize the above features, three novel underactuated mechanisms are proposed, as described in detail in the following subsections.

A. Shape Adaptation for Fingers

For the fingers to perform shape adaptation, an under-actuated mechanism based on a spring is proposed. In this mechanism, a spiral spring is adopted to allow for relative displacement of the fingers when an irregular object is grasped. To describe this idea clearly, a simplified schematic is illustrated in Fig. 1. In the metacarpophalangeal joints, each finger is connected to the corresponding spiral spring through a housing. The springs are also enclosed by the housing to reduce the required space and maintain deflection. In addition, the housing is supported by a holder to offer free-wheeling motion. The spiral spring is wound around and fixed to a shaft, which is actuated by a motor. In this structure, the motor's power can be transmitted to the shaft by a simple spur gear set.

Figure 2 shows the operation of the spiral spring when the KNU hand performs adaptive grasps. These operations are divided into four states according to the grasping mode: reaching, adaptation, power grasp, and release mode. (a) The reaching mode starts when the finger is fully extended and ends before the finger encounters an object. During this mode, the spiral spring has a small amount of deflection and transmits the motor's power to the finger with a small friction loss between the housing and the holder. (b) When the finger maintains contact with an object, the spiral spring is wound up and stores the motor's power. This operation then allows the other fingers to continue flexion. In this adaptation mode, the spring provides a grasping force proportional to the winding length. (c) The power grasp mode means that the grasping force directly depends on the motor's rotation. Here, the spiral spring is fully wound up to the shaft's constrained diameter, so the spiral spring and housing operate as a rigid

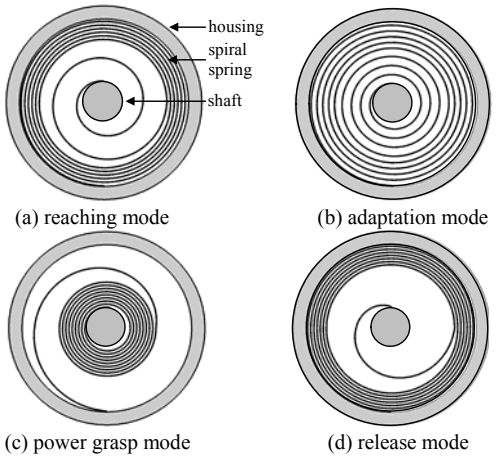

Fig. 2. Four operating modes of spiral spring.

wheel attachment for the shaft and finger. (d) In the release mode, the finger has no contact during operation and moves back to the initial extended position. The spring is unwound back to the housing's constrained diameter, in contrast to the power grasp mode. Thus, the finger can be extended by reverse rotation of the motor.

B. Self-locking for Fingers

Although the previous subsection proposed a spiral spring mechanism, the spring can be deflected by external forces that arise when the user moves their wrist or arm, or when an object's weight varies. The motor is also required to apply continuous torque to the fingers after the fingers adapt to an object. Conventional myoelectric hand usually provides a self-lock element located between the motor and the gear box to prevent rigid fingers from back-driving and conserve the battery power. However, this method is only available under limited condition when the fingers are simultaneously driven by a motor.

Thus, to cope with this problem, a new self-lock mechanism is proposed for each finger, as well as the motor, where a cam-ball mechanism is used to make a positive, quiet, one-way clutch. As shown in Fig. 3, the conventional cam-ball clutch consists of an inner member, outer member, and balls. The inner driving member has cam surfaces on the opposite side of the outer driving member and carries balls to either wedge or unwedge them. (a) During the counter-clockwise rotation of the inner member, self-energizing friction forces the balls to tightly wedge between the inner and outer members. As a result, the outer and inner members are driven in the same direction. (b) Conversely, if the inner member rotates clockwise or the outer member attempts to run ahead of the inner member, the balls are moved out of the tightly wedged position. Consequently the connection between the inner and outer members is broken.

Thus, using the principle of a cam-ball clutch, a self-lock element is proposed that allows unidirectional power transmission from the driving part to the driven part. To better explain this mechanism, a schematic of the proposed self-lock

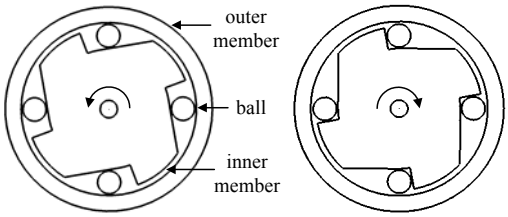

(a) clutching action (b) unclutching action

Fig. 3. Conventional cam-ball clutch.

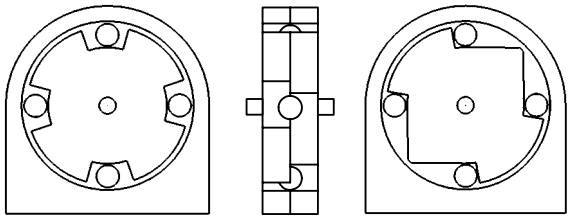

(a) driving plate side (b) driven plate side

Fig. 4. Cam-ball mechanism for self-locking.

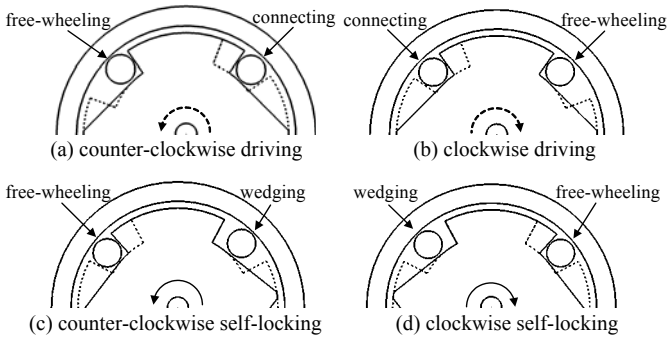

(a) counter-clockwise driving (b) clockwise driving

(c) counter-clockwise self-locking (d) clockwise self-locking

Fig. 5. Four operating modes of cam-ball mechanism.

is shown in Fig. 4. The self-lock is composed of a driving plate, driven plate, outer member, and balls. (a) The driving plate has cam surfaces with the same curvature as the outer member, and the distance between the cam surface and the inside of the outer rim is larger than the ball's diameter. (b) Meanwhile, in the driven plate, inclined cam surfaces are arranged symmetrically with respect to the horizontal and vertical axes. The outer member plays the role of a stationary holder and cooperates with the driven plate's inclined cam surfaces to impart a friction force to the balls.

The self-lock has four operating modes: driving in both directions and locking in both directions. Figure 5 illustrates how the self-lock mechanism performs these four operating modes to transmit power unidirectionally. In each schematic, the solid and dashed lines indicate the driven plate and driving plate, respectively, while the solid and dashed arrows denote the direction of each plate's rotation. (a) When the driving plate rotates counter-clockwise, the right ball lies between the edges of two cam surfaces and connects the two plates to transfer rotary power. Meanwhile, the left ball is in a free-wheeling state and has no influence on the rotation. As a result, this configuration prevents the balls from wedging and allows rotation with no friction. (b) In the reverse configuration, the elements are engaged in clockwise driving. (c) During the locking mode, an external torque is applied to the driven plate, whereas in the counter-clockwise case, the right ball is wedged between the inclined cam surface and the outer member, yet the left ball is not involved in the locking motion. This mechanism is based on the same principle as a one-way clutch. (d) Finally, locking in the reverse direction is similar to the case of counter-clockwise locking.

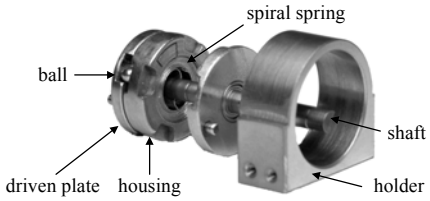

Fig. 6. Metacarpophalangeal joint.

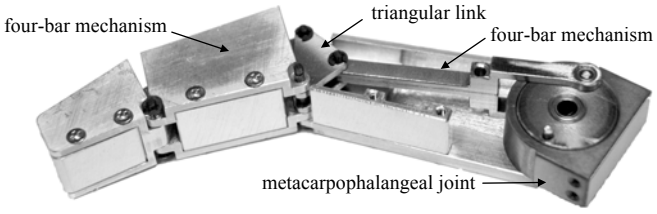

Fig. 7. Finger module.

C. *Metacarpophalangeal Joint Design*

Based on the spiral spring and cam-ball mechanism, a design for the metacarpophalangeal joint is proposed that includes shape adaptation and self-locking functions. To link these functions in a constrained space, the spiral spring's housing is designed to have the same cam surfaces as the self-locking element's driving plate. The driven plate is attached to the shaft through a bearing and has two hinge pins to connect each finger. Plus, two driven plates are located on both sides of the housing to improve the power transmission reliability and connectivity for the finger mechanism. Therefore, eight balls are engaged with the cam surfaces on both sides. Figure 6 shows an exploded view of the metacarpophalangeal joint. Using the same mechanism, another self-lock is embedded in the motor and connected to the shaft through the spur gear, allowing the spiral spring to store the motor's power without continuous driving.

D. *Finger Design*

Four fingers are required to facilitate adaptive grasping between phalanges. Thus, to satisfy this need, an underactuated finger is presented based on the seven-bar mechanism [4]. Figure 7 shows the proposed finger with a metacarpophalangeal joint. The finger has three degrees of freedom with three phalanges. To connect the proximal phalanx to the metacarpophalangeal joint, a modified seven-bar mechanism is used. By removing one bar, the end of the proximal four-bar mechanism is attached to the driven plate's hinge pins. The middle phalanx is composed of a four-bar mechanism and is coupled with the proximal phalanx through a triangular link to provide shape adaptation for the proximal interphalangeal joint. Also, an adaptive distal interphalangeal joint is achieved by connecting the distal phalanx to the end of the middle four-bar mechanism.

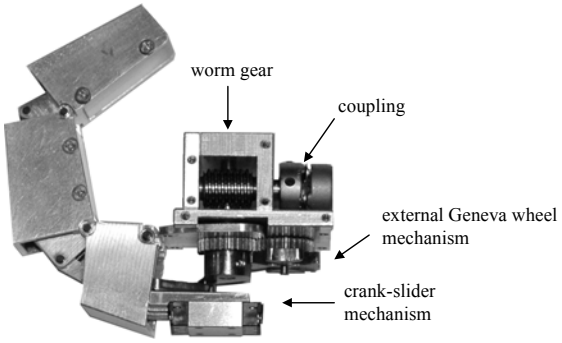

Fig. 8. Thumb module.

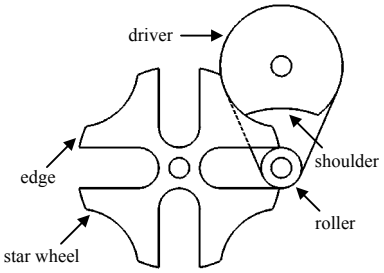

Fig. 9. External Geneva wheel mechanism.

During flexion motion, shape adaptation is achieved by a sequential contact of phalanges. Before the finger encounters an object, the three phalanges behave as one rigid link. When the proximal phalanx contacts an object, the middle then begins to flex and eventually meets the object. In the same way, the distal also performs shape adaptation. As a result, the three phalanges wrap the object with multi-point contacts.

E. Thumb Design

The KNU hand's thumb has four degrees of freedom. Like the fingers, it can perform adaptive grasping, and can adduct and abduct. Adduction and abduction are realized by means of an intermittent mechanism. This approach has been used in the Manus hand [5], where a timing gear provides cyclic movement. However, the interphalangeal joint is coupled with the carpometacarpal joint and a complex driven path is required to transmit the motor's power. Thus, to resolve this problem, a thumb design is proposed using an external Geneva and crank-slider mechanism. Figure 8 shows the complete thumb assembly. All the motions of the thumb are driven by a single motor, and a worm gear provides the actuation for the Geneva mechanism and self-locking for all the joints. The Geneva mechanism is composed of a star wheel, roller and driver (see Fig. 9). The roller is at the point of entering the slot and begins to drive the star wheel. Drive motion then ceases when the roller has moved through a 90-degree angle. The star is locked during its rest periods, as the concentric shoulder of the driver has engaged the corresponding edge of the star. The operation of this external Geneva mechanism is smoother than timing gears. As shown in Fig. 8, a spur gear set is used to transfer the intermittent rotary motion to the shaft for adduction and abduction. In the crank-slider mechanism, the Geneva wheel's diver is used as a crank and coupled with the slider through a connecting bar.

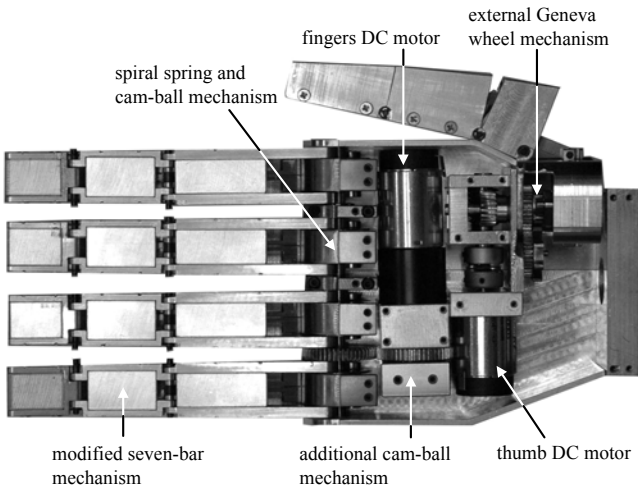

Fig. 10. KNU Hand.

TABLE I
SPECIFICATIONS OF KNU HAND

Components	Specifications
Dimensions (mm)	190L x 90W x 30H
Weight (g)	800
Degrees of freedom (DOFs)	16
Materials	Aluminum and stainless steel
Actuators	Two Maxon DC motors
Controller	TMS320F2812
Sensors	Two Murata potentiometers

As a result, the intermittent rotary motion is changed to a reciprocating linear motion. The thumb has three phalanges and a design similar to that of the fingers. Plus, the end of the proximal four-bar mechanism is connected to the slider to generate flexion and extension.

F. KNU Hand

A prototype of the KNU hand was fabricated according to the design concept described above. Figure 10 shows a palmar view of the KNU hand, except for the palm section; and its specifications are presented in Table 1. The hand is almost the same size as a male adult's hand and slightly heavier than a conventional myoelectric hand. In addition, the hand's appearance is similar to that of a human hand. Although the KNU hand has 16 degrees of freedom, it only uses two DC motors: one drives the four fingers with a 29:1 planetary gear, while the other actuates the thumb through a 20:1 worm gear. The frames are all made of light weight aluminum, whereas the self-lock element and gear set are fabricated using stainless steel for abrasion resistance. The hand motions are controlled by a digital signal processor (DSP) and pair of motor driver circuits. For position feedback, two small and flat potentiometers are attached to the shafts and wired to an analog-to-digital converter (ADC) embedded in the DSP. Based on its mechanical design features and control system, the KNU hand performs four grasping modes: cylindrical, tip, hook, and lateral grasps. These motion commands are generated by an EMG pattern recognizer and sent to the DSP controller via a serial communication interface, as described in detail in the following section.

III. EMG Pattern Recognition for KNU Hand

Since multifunction myoelectric hands have a number of degrees of freedom and dexterous hand functions, a robust and computationally efficient EMG pattern recognition method is required to classify and control these hand functions. In previous studies [6], [7], [8], the current authors proposed EMG pattern recognition methods for an independent actuated hand that had four DOFs, including pronation and supination, radial and ulnar flexion, flexion and extension, and open and grasp. Therefore, based on such previous results [8], this paper proposes a modified EMG pattern recognition that is suitable for the KNU hand with adaptive grasping capabilities.

A. Data Acquisition

The EMG pattern recognizer attempts to classify five kinds of hand motion: a cylindrical grasp, tip grasp, hook grasp, lateral grasp, and open. Thus, four surface electrodes are used to measure the EMG signals from the extensor digitorum, extensor carpi radialis, palmaris longus and flexor carpi ulnaris. Although the frequency range of an EMG signal is generally from 0 to 1000 Hz, the dominant energy is concentrated between 20 and 500 Hz, and the amplitude limited from 0 to 10 mV. Therefore, an active surface electrode was developed that included a bandpass filter with a 10 to 450 Hz bandwidth and an amplifier with a 60 dB gain. The EMG signals are digitized using an ADC, and the sampling frequency is 1024 Hz.

B. Feature Extraction

The preprocessing stage uses an overlapped moving window scheme, where each moving window is 250 ms long with a 125 ms increment. A combination of various features is extracted from each channel, where a feature set consists of fourth-order autoregressive coefficients and time domain statistics, including the number of zero crossings, waveform length, number of slope sign changes and mean absolute value. The feature set for each channel is an eight-dimensional feature vector, while the feature set for the four channels is a 32-dimensional feature vector.

C. Gaussian Mixture Model-based Classification

Consider the feature set $X = \{x^1, \ldots x^N\} \subset \Re^d$. The probability density function of a K -component Gaussian mixture model (GMM) is given by

$$p(x \mid \theta) = \sum_{k=1}^{K} p(k)\, p(x \mid \theta_k), \quad (1)$$

where $p(k)$ is the mixing probability and satisfies $p(k) \geq 0$ and $\sum_{k=1}^{K} p(k) = 1$. Each θ_k contains $\{\mu_k, \Sigma_k\}$ and the complete set of parameters is $\theta = \{p(k), \theta_k\}_{k=1}^{K}$, plus $p(x \mid \theta_k)$ denotes the Gaussian densities

$$p(x \mid \theta_k) = (2\pi)^{-d/2} \mid \Sigma_k \mid^{-1/2} \exp\left[-\frac{1}{2} (x - \mu_k)^T \Sigma_k^{-1} (x - \mu_k) \right]. \quad (2)$$

For the parameter estimates, a Bayesian regularization method is used to prevent a singular solution. A penalty term is added to the log-likelihood function as a regularizer. If the logarithm of a conjugate prior is chosen as the penalty function, expectation-maximization update rules can be derived to obtain the optimal parameter estimates. In the model order selection stage, a Bayesian-Laplace approximation is used to drive a data evidence equation, which represents the likelihood of data given the parameters, the prior parameter distribution, and the covariance of the posterior parameter distribution. Therefore, the conjugate prior distribution chosen in the parameter estimation stage can be used as a complexity penalty. As a result, the proposed method can find the optimal order of a GMM with enhanced stability.

A set of GMMs associated with five kinds of hand motion was constructed, where each motion is represented by a GMM referred to by $p(x \mid m)$, $m = 1, \ldots, 5$. During the learning procedure, for each GMM $p(x \mid m)$, parameter estimation and model order selection are performed using the proposed method and data for class m . In the performance evaluation, for a given feature vector, the maximum posterior was selected as the recognized motion using Bayes formula

$$p(m \mid x) = p(x \mid m)\, p(m) / p(x) \quad (3)$$

where $p(m)$ is the prior probability for class m . For this paper, it was assumed that each hand motion was generated from a flat distribution. Therefore, class m was identified as maximizing $p(x \mid m) \propto p(m \mid x)$.

D. Experimental Results

After determining the parameters and model orders in the learning procedure, the recognition accuracy of the proposed GMM classifier was evaluated. Figure 11 shows the four-channel EMG signals and recognized results. The subject performed five hand motions, which were switched in a random order. The GMM's maximum output was selected as the recognized motion in every decision. For the recognized results, each motion was assigned a number from 0 to 4, and a solid line and open circle used to denote the desired output and recognized motion, respectively. The results were stable for steady-state motions, yet not for transient-state motions. However, even if the proposed method had produced good results, analogous motions, such as cylindrical and tip grasps or hook and lateral grasps, generated a similar EMG pattern, causing different class features to be overlapped in the feature space, which would force the user to concentrate on hand control to prevent the generation of undesired motions. However, the KNU hand can solve this problem by adapting its grasping modes. In the KNU hand, although cylindrical and tip grasps and hook and lateral grasps use the same motion control algorithms, the grasping modes are automatically changed according to the shape of an object. Consequently, analogous EMG patterns can be classified as one motion, allowing the user to operate the hand naturally without any additional attention. Figure 12

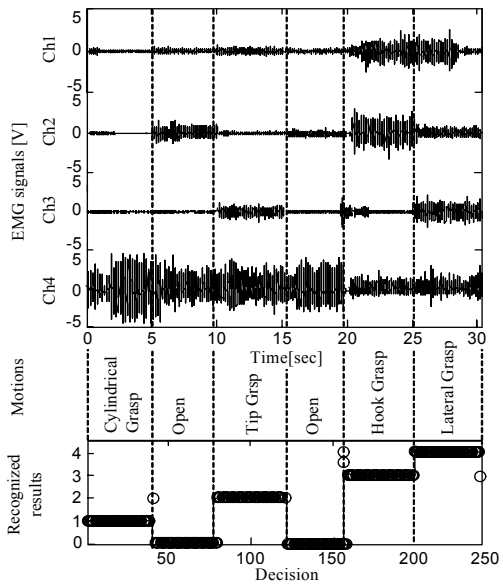

Fig. 11. EMG signals and recognition results.

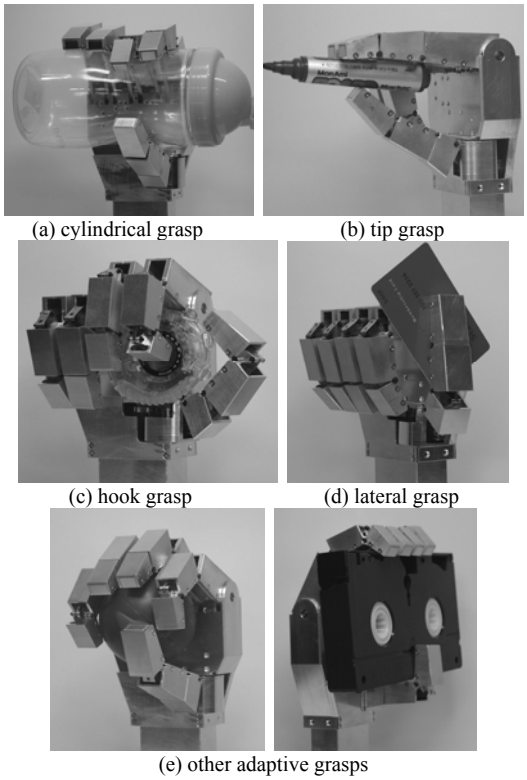

(a) cylindrical grasp (b) tip grasp

(c) hook grasp (d) lateral grasp

(e) other adaptive grasps

Fig. 12. Grasping motions of KNU hand.

shows the KNU hand controlled by EMG signals. The hand performed four grasping motions and was capable of adaptively grasping variously shaped objects.

Finally, an experiment was performed to test the self-locking of the proposed cam-ball mechanism. As a means of quantifying the self-locking performance, the grasping force was measured at the finger tips. Figure 13(a) shows the experimental setup where the KNU hand performed a tip grasp and an ATTONICS load cell was used to measure the grasping force. A steel plate was mounted on both the test bench and the load cell to provide the finger with

(a) experimental setup

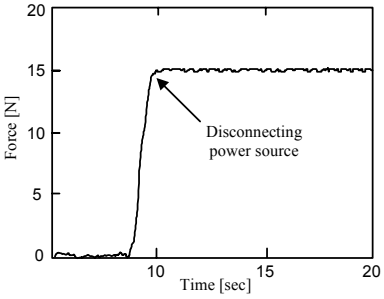

(b) grasping force

Fig. 13. Self-locking test and result.

a contact area to apply force, and the distance between the plates was set at 70 mm. The configuration of the joints was automatically determined by the adaptive grasping of the fingers and thumb. Figure 13(b) shows a typical response of the load cell during the tip grasping. After the force reached a predetermined value, the power source was disconnected from the motors. Nonetheless, the KNU hand maintained its grasping force due to the self-locking capability of the cam-ball mechanism.

IV. Conclusion

This paper presented a multifunction myoelectric hand to improve the grasping capabilities. The proposed hand design allowed adaptive grasping and self-locking using a spiral spring and cam-ball mechanism. Plus, GMM-based EMG pattern recognition classified four kinds of grasping motion, and controlled the KNU hand in real time.

References

[1] N. Dechev, W. L. Cleghorn, and S. Naumann, "Multiple finger, passive adaptive grasp prosthetic hand," *Mechanism and Machine Theory*, Vol. 36, pp. 1157-1173, 2001.

[2] P. J. Kyberd and J. L. Pons, "A comparison of the Oxford and Manus intelligent hand prostheses," in *Proc. IEEE Int'l Conf. Robotics and Automation*, 2003, pp. 3231-3236.

[3] M. C. Carrozza, C. Suppo, F. Sebastiani, B. Massa, F. Vecchi, R. Lazzarini, M. R. Cutkosky, and P. Dario, "The SPRING hand: Development of a self-adaptive prosthesis for restoring natural grasping," *Autonomous Robots*, Vol. 16, pp. 125-141, 2004.

[4] T. Laliberte and C.M. Gosselin, "Under-actuation in space robotic hands," in *Proc. 6th Int'l Symp. Artificial and Robotics & Automation in Space*, 2001, pp. 18-22.

[5] J. J. Pons, E. Rocon, R. Ceres, D. Reynaerts, B. Saro, S. Levin, and W. Van Moorleghem, "The MANUS-HAND Dextrous robotics upper limb prosthesis: Mechanical and manipulation aspects," *Autonomous Robots*, Vol. 16, pp. 143-163, 2004.

[6] J. U. Chu, I. Moon, and M. S. Mun, "A real-time EMG pattern recognition system based on linear-nonlinear feature projection for a multifunction myoelectric hand," *IEEE Trans. Biomedical Engineering*, Vol. 53, No. 11, pp. 2232-2239, Nov. 2006.

[7] J. U. Chu, I. Moon, Y. J. Lee, S. K. Kim, and M. S. Mun, "A supervised feature-projection-based real-time EMG pattern recognition for multifunction myoelectric hand control," *IEEE/ASME Trans. Mechatronics*, Vol. 12, No. 3, pp. 282-290, June 2007.

[8] J. U. Chu and Y. J. Lee, "Conjugate prior penalized learning of Gaussian mixture models for EMG pattern recognition," in *Proc. IEEE/RSJ Int'l Conf. Intelligent Robots and Systems*, 2007, pp. 1093-1098.